Solving problems with unilateral constraints by DAE methods

Martin Arnold* Kurt Frischmuth†

July 9, 1997

Abstract

We study trajectories of mechanical systems with unilateral constraints under the additional assumption that always a given number of constraints is active. A reformulation as problem with bilateral conditions yields a drastic reduction in the number of constraints, but in general, we are faced with regularity problems. We illustrate our approach in the special case of a dynamical rigid body contact problem. In particular, we present a regularization technique which leads to the definition of generalized solutions and a quite effective numerical method on the basis of algorithms for differential-algebraic systems. The results are applied to a wheel-rail contact problem of actual interest to railway engineers.

1 Introduction

In many physical problems an unknown time-dependent vector $q = q(t) \in \mathbb{R}^{n_q}$ is restricted to a given set $X_{\text{adm}} \subset \mathbb{R}^{n_q}$ of *admissible positions*, usually defined by a family of constraints

$$h(q;s) \geq 0 \quad \forall\, s \in S \subset \mathbb{R}^{n_s} \tag{1}$$

with $h : \mathbb{R}^{n_q} \times S \to \mathbb{R}^{n_h}$ (this inequality is to be read componentwise if $n_h > 1$).

If the equation of motion for the unconstrained problem is given by

$$\ddot{q} = \frac{d^2}{dt^2} q(t) = f(t, q, \dot{q}) \;, \tag{2}$$

then the constraints introduce a *reaction* $r(t, q, \dot{q})$ which acts in addition to f in order to keep q in X_{adm}. Usually this reaction vanishes if $q \in \operatorname{int} X_{\text{adm}}$, and it is an inner normal to ∂X_{adm} if $q \in \partial X_{\text{adm}}$. (We consider here scleronomic and ideal constraints only.)

We can obtain the special case $X_{\text{adm}} = X_0 = \{\, g(q;c) = 0 \;\; \forall\, c \in C \,\}$ by adding formally a negative counterpart to each of the unilateral constraints. With suitable regularity assumptions there will be no interior points, and any reaction normal to X_0 is possible.

In both cases we obtain an evolution problem of the form

$$\begin{array}{rcl} \ddot{q} & = & f(t, q, \dot{q}) + r \;, \\ q & \in & X_{\text{adm}} \;. \end{array} \tag{3}$$

We avoid here a general formalism for the description of r, throughout this paper it will be either a combination of a finite subfamily of the gradients $\nabla_q h(q;s)$, $s \in S$ (resp. $\nabla_q g(q;c)$,

*DLR Research Center Oberpfaffenhofen, Institute of Robotics and System Dynamics, P.O. Box 1116, D – 82230 Wessling, Germany, E-mail: martin.arnold@dlr.de

†University of Rostock, Department of Mathematics, P.O. Box, D – 18051 Rostock, Germany, E-mail: kurt@sun2.math.uni-rostock.de

$c \in C$) or a (nonlinear) function of such a combination. For mechanical systems this will be the sum of the classical term containing the Lagrange multipliers and a friction term which may have a complicated structure.

While for the special case of bilateral (or equality) constraints analysis and numerical methods are well studied there are still considerable problems in the general unilateral case. The aim of the present paper is to discuss a class of unilateral problems that can be transformed to bilateral ones using additional information about the considered model: we suppose that the trajectory $q(t)$ remains in $\partial X_{\mathrm{adm}}$ and, moreover, that for all n_h constraints there is always (at least) one $s \in S$ such that $h_i(\,\cdot\,; s)$ is active in $q(t)$, i. e.

$$\forall\, t \in [0,T] \quad q(t) \in X_{\mathrm{adm}} \quad \text{and} \quad \forall\, i \leq n_h \quad \exists\, s_i(t) \in S \;:\; h_i(q(t); s_i(t)) = 0\,. \tag{4}$$

This type of additional information is motivated by our main application: a rigid wheel (or wheelset) moving on a (standard) track. While the contact is obviously unilateral, in standard exploitation mode wheels have continuous contact with rails.[1] Thus we have $n_h = 1$ for a single wheel and $n_h = 2$ for a wheelset, the index i of $s_i(t)$ counts the possible regions of contact.

Let us consider a vector q such that each of the equations $h_i(q; s_i) = 0$ has exactly one solution $s_i = s_i(q)$. Then we obtain n_h equality constraints

$$0 = g(q) := h(q; s(q))\,, \tag{5}$$

i. e. a (possibly infinite) family of unilateral constraints is reduced to n_h bilateral constraints and problem (3) can be handled by standard techniques for differential-algebraic (DA) systems.

However, even if h is sufficiently differentiable the equality constraints (5) may be not differentiable because $s(q)$ might be discontinuous (in general $h(q; s) = 0$ even defines a multi-function $s(q)$). We show that in such cases classical solutions may not exist and introduce weak solutions as limits of solutions to regularized problems. The non-existence of classical solutions can be caused by the (in that case wrong) additional information, but it may also be inherited from the unilateral problem. In the application to wheel-rail systems the problem is genuine: caused by the fact that rigid contact is assumed where (at least) a transient deformation of wheel and rail is imperative. The idea of our procedure is to reintroduce such deformation, though to a very rudimental degree: just to remove the existence problem, but avoiding extra computational costs.

The paper is organized as follows: in Sec. 2 we consider the smooth case and summarize results for the numerical solution of this type of DA-systems. The ideas are illustrated by an example which leads to smooth bilateral constraints for certain parameters and to nonsmooth ones for others. In Sec. 3 we study this example in more detail and prove the non-existence of a classical solution in the nonsmooth case. The analysis of the transition through a wedge, that is carried out in Sec. 4, gives the basic motivation for a regularization of the model equations. In the final Sec. 5 we apply this regularization to the wheel-rail contact problem and compare the simulation results for the original and the regularized model equations.

2 Problems with unilateral constraints: the smooth case

Problems with unilateral constraints have been studied intensively in the context of the dynamical simulation of mechanical multibody systems with contact conditions. In this section we discuss analysis and numerical treatment of the model equations for the special case that the

[1] We neglect high frequency elastic vibrations that can violate this assumption, cf. [16].

equations $h(q;s) = 0$ are globally uniquely solvable w. r. t. s and define a sufficiently differentiable function $s = s(q)$.

We start this section with an example that will be used throughout the present paper to illustrate our approach. Similar examples have been studied by other authors (see e. g. [5]).

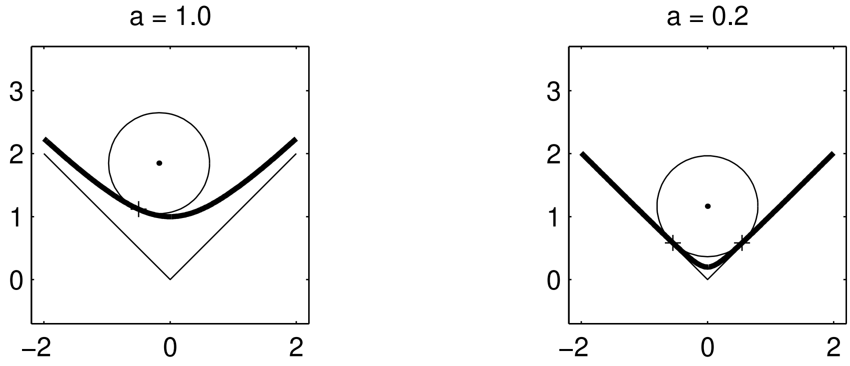

Figure 1: Disk moving on the floor $\eta = \sqrt{\xi^2 + a^2}$, ($\varrho = 0.8$).

Example 1 We consider the motion of a plane disk in $\mathbb{R}^2$ that is continuously in contact with the floor. This motion is described by (3) with $q \in X_{\text{adm}} \subset \mathbb{R}^3$. The components q_1 and q_2 of q are the two cartesian coordinates of the centre of mass, $q_3 = \alpha$ denotes the angle of rotation. f_1 and f_2 are the resulting force acting on the mass centre, f_3 is the angular momentum.
Let the contour of the rolling body be described by

$$(\xi - q_1)^2 + (\eta - q_2)^2 = \varrho^2 , \tag{6}$$

the "floor" is given by $\eta = u(\xi)$. We focus on the special case

$$u(\xi) = \sqrt{\xi^2 + a^2} \tag{7}$$

with a parameter $a > 0$. We have $u \in \mathcal{C}^\infty$ but in the limit case $a \to 0$ function u converges (pointwise) to $u_0(\xi) := |\xi|$, $u_0 \notin \mathcal{C}^1$.
The (unilateral) constraints are given by the condition that no point of the disk is allowed to be at any time below the floor. This condition for the positions q_1, q_2 may be expressed using the parametrization $\xi(s;q) = q_1 + \varrho \cos s$, $\eta(s;q) = q_2 + \varrho \sin s$ of the contour:

$$\forall\ s \in [0, 2\pi) \quad \eta(s;q) \geq u(\xi(s;q)) . \tag{8}$$

Obviously, no interior point of the body is below the ground if all points of the boundary satisfy the constraint. Let $q \in X_{\text{adm}}$ be given. If we have for (at least) one s equality in (8) then $q \in \partial X_{\text{adm}}$. Now, we strengthen the assumption introducing the additional information that the rolling body never leaves the ground, i. e. in addition to (8) we suppose

$$\exists\ s_0\ :\ \ \eta(s_0;q) = u(\xi(s_0;q)) . \tag{9}$$

At the moment we restrict ourselves to the case $a > \varrho$, i. e. the curvature of u is always smaller than the curvature of the disk surface. In this case a straightforward geometrical analysis proves that for given $q \in \partial X_{\text{adm}}$ the parameter s_0 in (9) is uniquely determined (see the left plot of Fig. 1): if $q \in \partial X_{\text{adm}}$ then we have obviously $s_0 \in (\pi, 2\pi)$ in (9) and

$$u'(\xi(s_0;q)) = \frac{d}{d\xi}(q_2 - \sqrt{\varrho^2 - (\xi - q_1)^2})\Big|_{\xi=\xi(s_0;q)} \tag{10}$$

(otherwise the surfaces of disk and floor would penetrate each other in a neighbourhood of $(\xi(s_0;q),\eta(s_0;q))$). For a given $q\in\partial X_{\rm adm}$ condition (10) can not be satisfied by more than one s_0 because

$$u''(\xi)\le\frac{1}{a}<\frac{1}{\varrho}\le\frac{d^2}{d\xi^2}(q_2-\sqrt{\varrho^2-(\xi-q_1)^2})\quad\forall\,\xi\in(q_1-\varrho,q_1+\varrho)\,.$$

This fact allows to substitute the infinite number of unilateral constraints (8) by one single bilateral constraint. On the boundary of the rolling body we introduce the elevation

$$\delta(s,q):=\eta(s;q)-u(\xi(s;q))=q_2+\varrho\sin s-\sqrt{(q_1+\varrho\cos s)^2+a^2}$$

above the floor (for geometrical reasons we can restrict ourselves to $s\in(\pi,2\pi)$). The parameter $s_c(q)$ of the minimizer is the candidate for the active constraint. Hence, we end up with one single constraint $\delta(s_c(q),q)=0$, i. e.

$$0=g(q):=\delta(s_c(q),q)=q_2+\varrho\sin s_c(q)-\sqrt{(q_1+\varrho\cos s_c(q))^2+a^2}\,. \tag{11}$$

The set of all positions q satisfying this strengthened constraint will be referred to as admissible manifold $\mathfrak{M}$. Here, we have to express s_c in terms of derivatives of the parametrization and the floor. We obtain $s_c(q)$ as the unique solution of $\delta_s(s,q)=0$. (Because of the special structure of δ the derivative $\delta_s(s,q)$ is independent of q_2 and q_3 such that $s_c=s_c(q_1)$ and (11) defines q_2 as function of q_1).

Guided by this example more complicated problems with unilateral constraints can be transformed to equivalent problems with n_h equality constraints provided that

- the additional assumption (4) is satisfied and
- there is a function $k:\mathbb{R}^{n_q}\times S\to\mathbb{R}^{n_s}$ such that $k(q;s)=0$ is *globally* uniquely solvable w. r. t. $s\in S$ and

$$k(q;s_c)=0\,,\;\;h(q;s_c)=0\quad\Rightarrow\quad h(q;s)\ge 0\;\;\forall\,s\in S$$

("the smooth case"). In the above example we have $n_h=n_s=1$, $S=(\pi,2\pi)\subset\mathbb{R}$, $h=\delta$, and $k=\delta_s=\nabla_s\delta$.

In the smooth case our problem is equivalent to a DA-system with algebraic equations $k(q;s)=0$, $h(q;s)=0$, that may be substituted by one equality constraint $0=g(q)$ with

$$g(q):=h(q,s_c(q))$$

such that the auxiliary variables s are eliminated. In this section we apply recent results to the perhaps best understood equations of this type, the Euler–Lagrange equations for constrained mechanical motion in the more general form

$$\begin{aligned} M(q)\ddot q &= \varphi(t,q,\dot q,s,\lambda)-J(q,s)\lambda\,,\\ 0 &= k(q,s)\,,\\ 0 &= h(q,s)\,. \end{aligned} \tag{12}$$

Here q denotes the position coordinates, $s\in S$ are the coordinates of contact points and λ the Lagrange multipliers which couple the constraints to the dynamical equations via matrix

$$J:=(\nabla_q g)^T=(\nabla_q h-\nabla_s h\,(\nabla_s k)^{-1}\,\nabla_q k)^T\,.$$

$M(q)$ denotes the mass matrix and $\varphi(t, q, \dot{q}, s, \lambda)$ the resulting forces that may depend on λ (in the case of friction forces). We suppose that $\nabla_s k$ is non-singular in a neighbourhood of a solution of (12) such that the Implicit Function Theorem may be applied to solve $k(q, s) = 0$ w. r. t. $s = s_c(q)$. With the standard regularity assumption

$$\text{“} \begin{pmatrix} M(q) & J(q, s_c(q)) - \varphi_\lambda(t, q, \dot{q}, s_c(q), \lambda) \\ J^T(q, s_c(q)) & 0 \end{pmatrix} \quad \text{is non-singular ”} \tag{13}$$

Eqs. (12) form a DA-system of index 3 provided that the functions M, J, φ, k, h, and g are sufficiently differentiable (e. g. [12, Section VI.5]). Note, that

$$\nabla_q g = \nabla_q h - \nabla_s h \, (\nabla_s k)^{-1} \, \nabla_q k = J^T$$

simplifies substantially if function k is defined by $k(q, s) = \nabla_s h(q, s)$ as in Example 1 since $k(q, s) = 0$ implies then $\nabla_q g = \nabla_q h$, i. e. $J = (\nabla_q h(q, s))^T$.

It is well known that the analytical solution of (12) satisfies not only the original constraints $k(q, s) = 0$, $h(q, s) = 0$ on position level but also the *hidden constraints*

$$\begin{aligned} 0 &= \frac{d}{dt} k(q(t), s(t)) = \nabla_q k \cdot \dot{q}(t) + \nabla_s k \cdot \dot{s}(t) \,, \\ 0 &= \frac{d}{dt} h(q(t), s(t)) = \nabla_q h \cdot \dot{q}(t) + \nabla_s h \cdot \dot{s}(t) = J^T(q, s) \dot{q}(t) \,, \qquad (14) \\ 0 &= \frac{d^2}{dt^2} k(q(t), s(t)) \,, \quad 0 = \frac{d^2}{dt^2} h(q(t), s(t)) \qquad (15) \end{aligned}$$

on the levels of velocity and acceleration coordinates, respectively. With assumption (13) Eqs. (15) and (12) can be solved w. r. t. λ, i. e. for given q, $\dot{q}$ the variables s and λ are uniquely defined, $s = s_c(q)$, $\lambda = \lambda(t, q, \dot{q})$. Inserting these expressions into the dynamical equations $M\ddot{q} = \varphi - J\lambda$ of (12) a second order system of ordinary differential equations (ODEs) is obtained that is analytically equivalent to the DA-system. With this transformation it can be proven that under suitable assumptions an initial value problem for (12) is uniquely solvable if the initial values are *consistent* with the (original and hidden) constraints, i. e. if $g(q_0) = 0$, $J^T(q_0, s_0)\dot{q}_0 = 0$, $s_0 = s_c(q_0)$, $\lambda_0 = \lambda(t_0, q_0, \dot{q}_0)$ ([20]).

In principle also the numerical solution of (12) could be based on the transformation to an equivalent system of ODEs that may be solved by any standard ODE-solver. However, this approach requires the computation of $s_c(q)$ and $\lambda(t, q, \dot{q})$ whenever the right hand side of the ODE has to be evaluated. The numerical effort can be reduced substantially by applying a discretization method to the DA-system (12) directly (see the monograph [4] for the discussion of various applied problems). To avoid numerical instability we have to use in addition to (12) at least one of the hidden constraints (14), (15) in the numerical solution of the index-3 system (12), ([12, p. 483ff]).

There is a great variety of discretization methods in multibody system dynamics, see [5] for a comprehensive comparison. In the actual computations we apply BDF or (implicit) Runge–Kutta discretizations to

$$\begin{aligned} M(q)(\dot{q} - v) + J(q, s)\hat{\lambda} &= 0 \,, \\ M(q)\dot{v} + J(q, s)\lambda &= \varphi(t, q, v, s, \lambda) \,, \\ 0 &= k(q, s) \,, \\ 0 &= h(q, s) \,, \\ 0 &= J^T(q, s) v \,. \end{aligned} \tag{16}$$

This formulation generalizes the Gear–Gupta–Leimkuhler formulation of the model equations ([11], [2]), it avoids the (often very time-consuming) evaluation of (15). $\hat{\lambda}$ denotes some auxiliary variables that vanish identically for the analytical solution, i. e. $v = \dot{q}$.

In the dynamical simulation of wheel-rail systems this approach was applied by Simeon et al. to idealized systems with conic wheels ([21]). The combination of a rigid contact model (with equality constraints) and a discretization that is based on the DAE formulation yields a very efficient simulation tool.

3 More about the model problem

Motivated by the positive experience in the smooth case similar approaches have been studied in the general setting of problems (3). Already in the very simple model problem of Example 1 there are, however, essential differences to the smooth case. To discuss the *nonsmooth* case in more detail we consider in the beginning of this section some analytical solutions of the model problem in the *smooth* case. In a second part the discontinuities in the *nonsmooth* case are analysed and the relation to "impasse points" in DA–systems is studied.

We start this section with some additional notations: In the model problem of Example 1 the constraint $g(q) = 0$ is independent of $q_3 = \alpha$ and may therefore be rewritten as

$$\hat{g}(q_1, q_2) := g(q) = 0 \tag{17}$$

(see (11)). We denote by $\vec{n}$ the normed gradient of $\hat{g}$ and by $\vec{t} = (t_1, t_2)^T$ the vector that is obtained rotating $\vec{n}$ by $-\pi/2$. Eq. (17) defines the curve

$$\hat{\mathfrak{M}} := \{ (q_1, q_2) \,:\, \hat{g}(q_1, q_2) = 0 \} \subset \mathbb{R}^2 \ .$$

In the smooth case $(a > \varrho)$ this curve $\hat{\mathfrak{M}}$ is continuously differentiable. The arclength of $\hat{\mathfrak{M}}$ is given by $d\sigma = \sqrt{dq_1^2 + dq_2^2}$ such that the curvature κ satisfies

$$\kappa = \frac{d\beta}{d\sigma} \qquad \text{with} \qquad \beta := \arctan\left(\frac{t_2}{t_1}\right)$$

denoting the angle of the slope. Note, that we have for the model problem $\kappa > 0$ since (17) defines q_2 as convex function of q_1.

The equations of motion for a disk of radius ϱ, mass m and moment of inertia I are obtained from the balance of linear momentum

$$m \begin{pmatrix} \dot{v}_1 \\ \dot{v}_2 \end{pmatrix} = F_{\text{pot}} + F_{\text{con}} + F_{\text{fric}} \tag{18}$$

and the balance of angular momentum

$$I\dot{\omega} = \varrho\, F_{\text{fric}} \cdot \vec{t} \tag{19}$$

where we have used the notations $v = \dot{q}$, $\omega = \dot{\alpha} = \dot{q}_3$. The potential, constraint, and friction forces are denoted by F_{pot}, F_{con}, and F_{fric}, respectively. Since we are mainly interested in the transitions through singularities and these transitions mostly happen in vanishing time we neglect in the following the potential forces: $F_{\text{pot}} = 0$. For the friction law we make the simplest possible choice — Coulomb's law, setting

$$F_{\text{fric}} = -\mu \,\text{sgn}\, (v_{\text{slip}})\, |F_{\text{con}}|\, \vec{t} \tag{20}$$

with the friction coefficient μ and the relative speed

$$v_{\text{slip}} = v \cdot \begin{pmatrix} \vec{t} \\ \varrho \end{pmatrix} \tag{21}$$

between disk and floor at the contact point.

According to d'Alembert's principle the reaction to the ideal scleronomic constraint (17) is a force normal to $\hat{\mathfrak{M}}$

$$F_{\text{con}} = \lambda \vec{n}\ , \quad |F_{\text{con}}| = \lambda\ .$$

With these assumptions (18), (19), and (11) can be rewritten as model equations in standard form

$$\begin{aligned} \operatorname{diag}(m, m, I)\, \ddot{q} &= \begin{pmatrix} F_{\text{pot}} \\ 0 \end{pmatrix} + \lambda \begin{pmatrix} \vec{n} \\ 0 \end{pmatrix} - \mu \operatorname{sgn}(v_{\text{slip}})|\lambda| \begin{pmatrix} \vec{t} \\ \varrho \end{pmatrix}\ , \\ 0 &= g(q)\ . \end{aligned} \tag{22}$$

Note that for a (circular) disk there is no angular momentum as reaction to the constraint because g does not depend on q_3 (see (17)), or, by a physical argument, because the normal force points exactly to the center of mass. This feature is obviously lost for other shapes of the roller.

We remark that the normal and tangential directions are identical for floor and center of mass locus. Therefore the velocities $(v_1, v_2)^T$ can be written as

$$\begin{pmatrix} v_1 \\ v_2 \end{pmatrix} = v_t \vec{t} \qquad \text{with} \qquad v_t := \operatorname{sgn}(v_1) \cdot \sqrt{v_1^2 + v_2^2}\ .$$

This speed v_t is used to obtain the speed of slip at the contact point

$$v_{\text{slip}} = v_t + \varrho\, \omega \tag{23}$$

that determines the direction of the friction force (see (20) and (21)).

One key observation is that Eqs. (22) have a first integral:

$$\frac{d}{dt}(m v_t - \frac{1}{\varrho} I \omega) = m \dot{v}_t - \frac{1}{\varrho} I \dot{\omega} = F_{\text{fric}} \cdot \vec{t} - \frac{1}{\varrho}\, \varrho\, F_{\text{fric}} \cdot \vec{t} = 0\ ,$$

i. e. the quantity

$$m v_t - \frac{1}{\varrho} I \omega =: C \tag{24}$$

is preserved during the motion of the disk and can be used to compute ω for a given speed v_t.

Since we have assumed $F_{\text{pot}} = 0$ the equation for v_t can be solved straightforwardly as long as v_{slip} does not change its sign. If v_{slip} remains e. g. always positive then we obtain multiplying (18) by $\vec{n}$

$$\lambda = m v_t^2 \kappa$$

and therefore

$$\begin{aligned} \dot{v}_t &= -\mu \kappa v_t^2 \\ \frac{d v_t}{d\sigma}\, v_t &= -\mu\, \frac{d\beta}{d\sigma}\, v_t^2 \\ \ln |v_t| &= -\mu(\beta - \beta_0) \\ v_t &= v_{t,0} \cdot \exp(-\mu(\beta - \beta_0))\ . \end{aligned} \tag{25}$$

This gives us the actual speed and spin of the disk as functions of the initial values. If the initial slip is positive, speed is damped by the factor $\exp(-\mu(\beta-\beta_0))$. If the slip initially is negative, speed is increased by the inverse factor $\exp(\mu(\beta-\beta_0))$, i. e., kinetical energy is transferred from rotation into translation. In both cases the corresponding spin is obtained from the first integral C.

Up to now we have assumed that v_{slip} does not change its sign but from (23) and (24) we see

$$v_{\text{slip}} = v_t + \varrho\,\omega = v_t + \varrho^2\,\frac{mv_t - C}{I} = v_{\text{slip,o}} + (1+\frac{m\varrho^2}{I})(v_t - v_{t,0})$$

such that v_{slip} vanishes iff

$$v_t = v_{t,0} - \frac{I}{I+m\varrho^2}\,v_{\text{slip,o}}\,.$$

If $v_{\text{slip,o}} = 0$ is reached then the transfer of energy between rotational and translational mode ceases abruptly. Due to the lack of external forces we end up with

$$\begin{aligned} v_t &= v_{t,0} - \frac{I}{I+m\varrho^2}\,v_{\text{slip,o}} = \text{const} \\ \omega &= -\varrho^{-1}\,v_t = \text{const} \end{aligned}$$

and one degree of freedom is lost. In Fig. 2 we see for a disk passing a wedge with $\beta-\beta_0 = \pi/2$ the speed v_t versus $v_{t,0}$ and μ.

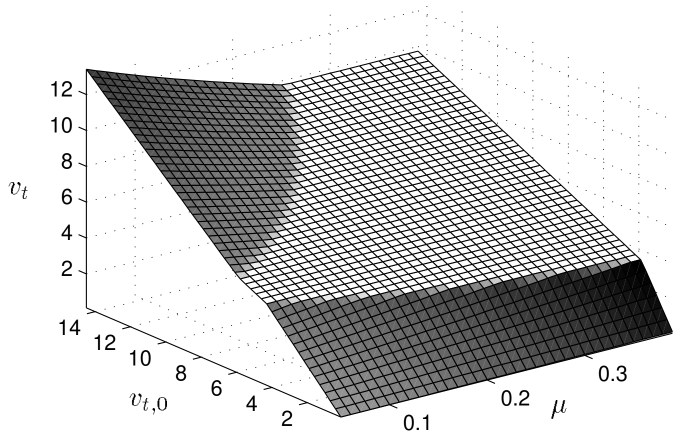

Figure 2: Wedge characteristic for $\omega_0 = -5$ and $\Delta\beta = \beta - \beta_0 = \pi/2$.

The very detailed knowledge about the model problem is not only useful in the smooth case (the smoothness of $\hat{\mathfrak{M}}$ is one of the basic assumptions of the above analysis) but can be used also to regularize the model equations in the nonsmooth case (see Section 4). Up to the end of this section we will discuss this nonsmooth case that is characterized by $a < \varrho$ for the model problem (if $a \geq \varrho$ then $\delta_s(s,q) = 0$ is globally uniquely solvable w. r. t. $s \in (\pi, 2\pi)$).

If $q_1 = 0$ then the common points of disk surface and floor are symmetric w. r. t. the η–axis (see the right plot of Fig. 1), i. e. $\delta_s(\pi+\tilde{s},q) = 0$ and $q_1 = 0$ imply $\delta_s(2\pi-\tilde{s},q) = 0$. In the case $a < \varrho$ we obtain by straightforward transformations from $q_1 = 0$

$$\delta_s(s,q) = 0 \quad \Leftrightarrow \quad (\ s = 3\pi/2 \quad \text{or} \quad \cos s = \sqrt{(\varrho^2 - a^2)/2\varrho^2}\ \ )$$

and the common points $(\xi(s_c(q);q), \eta(s_c(q);q))$ of disk surface and floor in the right plot of Fig. 1 are $(-\hat{\xi}, u(-\hat{\xi}))$ and $(\hat{\xi}, u(\hat{\xi}))$ with

$$\hat{\xi} := \varrho \cos s = \sqrt{(\varrho^2 - a^2)/2}\,, \quad u(\hat{\xi}) = u(-\hat{\xi}) = \sqrt{(\varrho^2 + a^2)/2}\,.$$

If $q_1 \neq 0$ then the common point is uniquely defined, it satisfies

$$\xi(s_c(q);q) \leq -\hat{\xi} \ \ (\text{if } q_1 < 0) \quad \text{and} \quad \xi(s_c(q);q) \geq \hat{\xi} \ \ (\text{if } q_1 > 0)\,.$$

Furthermore the vector $\vec{t}$ is tangential to the floor in $\xi(s_c(q);q)$ if $q_1 \neq 0$. This results in

$$\tan(t_2/t_1) \leq -\hat{u}' \ \ (\text{if } q_1 < 0) \quad \text{and} \quad \tan(t_2/t_1) \geq \hat{u}' \ \ (\text{if } q_1 > 0)$$

since u is convex and $\hat{u}' := u'(\hat{\xi}) = -u'(-\hat{\xi})$. Because of $\hat{u}' \neq 0$ and $v = v_t \vec{t}$ any trajectory $(q(t), \dot{q}(t))$ with $\lim_{t \to \hat{t}-0} q_1(t) = 0$ and $\lim_{t \to \hat{t}-0} \dot{q}_1(t) = \dot{q}_1^- \neq 0$ has a discontinuous velocity v at $t = \hat{t}$. This requires an impulsive force at $t = \hat{t}$.

For problem (3) we expect similar difficulties whenever the trajectory passes a state $\hat{q} \in \mathfrak{M}_0$ with

$$\mathfrak{M}_0 := \{\, \hat{q} \in X_{\mathrm{adm}} \,:\, \exists\, s_1, s_2 \in S,\ s_1 \neq s_2,\ h(\hat{q};s_1) = h(\hat{q};s_2) = 0 \,\}\,. \tag{26}$$

In general, these problems can not be solved by the techniques that were used in the smooth case in Sec. 2. We want to point out, however, that the difficulty is caused by the *analytical* nature of the problem and *not* by the numerical method.

Remark 1 a) In [17] we considered the dynamical simulation of a rigid wheelset with *wear profile* that results in model equations with nonsmooth constraints (see also Section 5). As long as $q(t) \notin \mathfrak{M}_0$ the numerical solution can be computed as in the smooth case. Using appropriate switching functions the time instances $\hat{t}$ with $q(\hat{t}) \in \mathfrak{M}_0$ can be determined efficiently during the numerical integration ([4, Section 5.3.3]). The crucial point, however, are the changes of $\dot{q}(t)$ if the trajectory passes $\mathfrak{M}_0$ at time $\hat{t}$. At $\hat{t}$ the integration has to be stopped, it could be continued for $t > \hat{t}$ with initial values $q(\hat{t}+0) = q(\hat{t}-0)$ and $\dot{q}(\hat{t}+0)$ if we would know how $\dot{q}(t)$ changes at $\hat{t}$. Until now we are not aware of a reasonable physical model that describes the jump $\dot{q}(\hat{t}-0) \to \dot{q}(\hat{t}+0)$ in this applied problem. So we end up with simulation results that may be far from physical reality (see Example 4).

b) If $a < \varrho$ then trajectories reaching a point $P^* = (q, \dot{q}, \lambda)$ with $q_1 = 0$ and $\dot{q}_1 \neq 0$ can not be extended continuously beyond this point P^*. Therefore these points P^* can not be passed by classical solutions, they are *impasse points* in the classical sense of this term. Note, however, that these singularities are caused by the non-differentiability of the constraint $g(q) = 0$ and *not* by a rank decay of a Jacobian. Impasse points that result from a rank decay of the Jacobian have been studied intensively in the literature (see e. g. [19]). In the early 1990s Führer observed that DA-systems (12) may have impasse points if k_s becomes singular ([10]). In our context of the original problem (3) the analysis of singularities in (12) would, however, be misleading since (3) and (12) are equivalent only, if the solution $q(t)$, $\dot{q}(t)$ satisfies *all* constraints (1), i. e. if $q \in X_{\mathrm{adm}}$. Example 2 below illustrates that impasse points of the DA-system (12) typically do not belong to X_{adm}, therefore they are of no interest for problem (3).

Example 2 Fig. 3 illustrates the relation between problems with unilateral constraints and the impasse points of the DA-system (12) in the case $a < \varrho$. The solid lines of the plots show $\xi(s_c(q);q)$ versus q_1 in the case $a > \varrho$ (Example 1) and $a < \varrho$, respectively. The dashed line in the right plot shows additionally all points $\xi(s;q)$ with $\delta_s(s,q) = 0$ and $s \neq s_c(q)$. At $q_1 = 0$

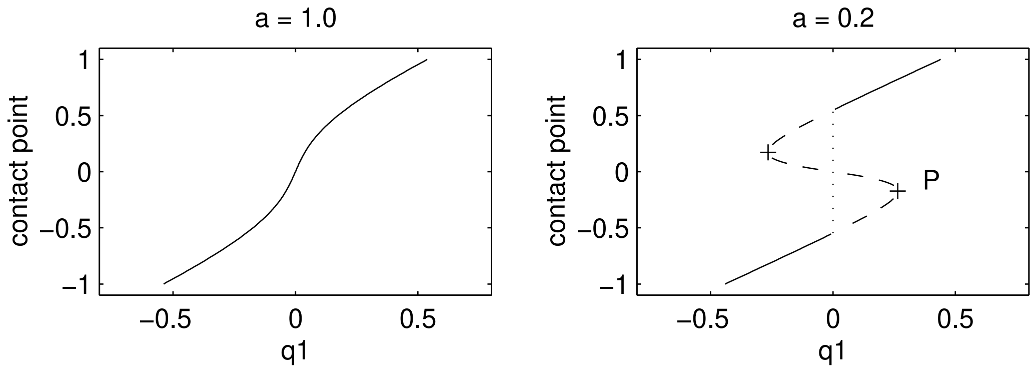

Figure 3: Point of contact between wheel ($\varrho = 0.8$) and floor.

the contact point coordinate $\xi(s_c(q); q)$ jumps from $-\hat{\xi}$ to $\hat{\xi}$. The solid lines mark X_{adm}, solid and dashed lines together mark all states with $\delta_s(s, q) = 0$ (i. e. $k(q, s) = 0$ in (12)). In the smooth case (left plot) Eqs. (3) are equivalent to (12) for all $(q, \dot{q}) \in \mathbb{R}^6$, there are no impasse points.
The solution of (12) follows continuously the line $\{(q_1, \xi(s; q)) : \delta_s(s, q) = 0\}$, in the case $a < \varrho$ (right plot) a trajectory with strictly monotonically increasing $q_1(t)$ and initial values $q_1(0) < 0$, $s(0) = s_c(q(0))$ on the solid line will therefore leave the solid line and follow the dashed line at $q_1 = 0$. Because of the turning point the trajectory can never pass point P. In P the derivative δ_{ss} (i. e. k_s) vanishes, the DA-system (12) has not longer index 3, so P is an impasse point for (12) with a rank decay of the Jacobian k_s. For the original problem (3) point P is, however, *no* critical point because it corresponds to a vector $q \notin X_{\text{adm}}$. The equivalence between (3) and (12) was lost when the trajectory passed $q_1 = 0$.

4 Transition through singularities and the basic concept of regularization

In this section we consider a regularization of the model equations in the nonsmooth case that is based on a detailed study of the transition through singularities in the model problem with $a < \varrho$.

Evidently, the center of mass of the disk is constrained to the union of two smooth branches:

$$\mathfrak{M} = \mathfrak{M}_- \cup \mathfrak{M}_+ = \{ q \in \mathfrak{M} \, : \, q_1 \leq 0 \} \cup \{ q \in \mathfrak{M} \, : \, q_1 \geq 0 \}$$

where the indices correspond to the sign of q_1. Both branches coincide at $q_1 = 0$, but they intersect at a non-vanishing angle $\Delta\beta$. In fact, since the floor $u(\xi)$ approximates $|\xi|$, the center of mass is elevated by about $\sqrt{2}\,\varrho$ (limit with $a \to 0$), the function $q_2 = q_2(q_1)$ tends to $|q_1| + \sqrt{2}\,\varrho$ (but again only in C^0).

Note that $\Delta\beta = \pi/2$ in the limit case ($a \to 0$). For $0 < a < \varrho$ we have $0 < \Delta\beta < \pi/2$, and $\Delta\beta$ is monotonous in a. Further, for q_2 there exists a unique decomposition of the form

$$q_2(q_1) = \tan\left(\frac{\Delta\beta}{2}\right) |q_1| + \tilde{q}_2$$

where $\tilde{q}_2$ is smooth. The set $\mathfrak{M}_0$ consists here of a line

$$\mathfrak{M}_0 = \{ q \in \mathfrak{M} \, : \, q_1 = 0 \} .$$

If $a < \varrho$ then it does not make sense to consider the equations of motion at $q \in \mathfrak{M}_0$ in their differential formulation, since they can not be solved by a function $q \in \mathcal{C}^1$. There is even no weak formulation within the classical theory of distributions that yields a unique solution for trajectories passing through $q \in \mathfrak{M}_0$. A unique solution can be obtained, only, by additional information on the nature of the modelled process.

In fact, in the first equation of (12) we have a product of a jump function J by a Dirac–distribution λ which is not defined within Schwartz' theory of distributions. For all pairs of distributions q, λ for which the right-hand side of that equation would be defined that right-hand side would be necessarily a classical function whereas the left-hand side contains obviously a non-vanishing multiple of the Dirac–distribution if $\dot{q}_1 \neq 0$, (cf. [22]).

This lack of uniqueness corresponds to the fact that physically each of the following cases can occur:

a) the disk bounces back onto the branch where it came from,

b) the disk gets stuck in the wedge,

c) the disk looses contact – at least temporarily,

d) the disk passes through the wedge.

The actual behaviour of the real physical system depends on the details of the physical realization of the constraints near the singularity. Further, this may be also influenced by the actual speed, by the angle $\Delta\beta$ and by material constants of floor and disk which do not enter the equations of motion on smooth parts of the constraint manifold $\mathfrak{M}$. We expect the behaviour of case a) if $\Delta\beta = \pi/2$ and the material is highly elastic, case b) would be expected if $\Delta\beta \approx \pi$ and the material is soft (e. g. visco-elastic).

In the following we will consider case d) in more detail. In particular, we postulate

$$\mathrm{sgn}\ (v_{1,-}) = \mathrm{sgn}\ (v_{1,+})$$

where $v_{1,-}$ and $v_{1,+}$ are the horizontal velocities before and after the jump (one-sided limits for $t \to \hat{t}$ where $q(\hat{t}) \in \mathfrak{M}_0$).

Remark 2 For our main application (wheel-rail systems) the velocity splits into a component orthogonal to the wedge and one parallel to it. Our assumption applies than to the orthogonal component. Practically, the parallel component is much larger, the approach to the wedge comparatively slow. That means that the deflection of the direction of the motion is rather small, so that the neglection of bouncing is a good approximation to the real situation. However, there are (especially constructed) examples where the wedge is attracting, i. e. after certain passages through $\mathfrak{M}_0$ (each time loosing normal speed) the trajectory eventually remains (practically) in the wedge — such cases correspond to b), cf. Example 4 of Sec. 5.

We conclude that the model equations for the motion along smooth branches need to be augmented by an additional *wedge model* for the transition through the singular points. Such a model can be given either by using a higher resolution theoretical approach — say by imbedding into a family of elastic problems, or by a phenomenological approach, i. e. by describing a relation between v_-, v_+ and certain parameters corresponding to the geometry and material features of the wedge.

Following [9], [7], [8] we present here a phenomenological model which parallels certain features of an elastic model. However, this approach is designed to be much faster than the actual solution of elastic contact problems. For the formulation of our phenomenological approximation, we preserve the following main features of an elastic model:

- Contact does not occur in an isolated point, but rather on a set of non-vanishing measure (the *contact patch* — which may be connected or not).
- In a motion from $\mathfrak{M}_-$ to $\mathfrak{M}_+$ the direction of motion changes gradually, not abruptly, while the component of the contact patch connected with $\mathfrak{M}_+$ grows and the original component (that is connected with $\mathfrak{M}_-$) decays.

However, in contrast to a pure elastic model the phenomenological model does not couple size, form and evolution of the contact patches directly to the equations of motion, i. e. to the normal force or the Lagrange multipliers since reasonable constants of elasticity (Young moduli $E = \mathcal{O}(10^{11}\,\mathrm{Nm}^{-2})$) would result in rather stiff systems that are difficult to solve numerically.

Instead we define close to $\mathfrak{M}$ new smooth constraint manifolds $\mathfrak{M}^{(\nu)}$ with a positive regularization parameter $\nu \ll 1$. The analysis that was carried out for the model problem in Section 3 allows to study the effect of the substitution $\mathfrak{M} \to \mathfrak{M}^{(\nu)}$ on the solution of the model equations:

Theorem 1 *Let* $\{\mathfrak{M}^{(\nu)} \,:\, \nu > 0\}$ *be a family of smooth cylindrical manifolds*

$$\mathfrak{M}^{(\nu)} = \{q \,:\, q_2 = \gamma^{(\nu)}(q_1)\}$$

where the scalar functions $\gamma^{(\nu)}$ *converge for* $\nu \to 0$ *pointwise to*

$$\gamma(q_1) := \max_{s\in(\pi,2\pi)} (-\varrho \sin s + \sqrt{(q_1 + \varrho\cos s)^2 + a^2}) \tag{27}$$

(see (11)), each of them coincides with γ *outside an interval* $[-\nu, \nu]$ *and is strictly convex in* $[-2\nu, 2\nu]$. *Furthermore, the forces in (18) are supposed to satisfy* $F_{\mathrm{pot}} = 0$ *and (20).*
Consider a family of trajectories approaching $\mathfrak{M}_0$ *at given velocities* $v_-^{(\nu)}$ *and leaving it with velocities* $v_+^{(\nu)}$.

a) If there is a limit $v_- = \lim_{\nu\to 0} v_-^{(\nu)}$ *then there exists a unique limit* $v_+ = \lim_{\nu\to 0} v_+^{(\nu)}$.

b) In this case v_+ *is independent of the family* $\{\mathfrak{M}^{(\nu)} \,:\, \nu > 0\}$ *, it is uniquely defined by* $\mathfrak{M}$*, i. e. by* γ*.*

Proof The analysis of Section 3 can be extended straightforwardly to the case $\nu > 0$ since $\gamma^{(\nu)}$ is supposed to be strictly convex. Therefore the statement of the theorem is a consequence of the explicit expression (25) that was obtained for the solution of the model problem. ■

Remark 3 a) Theorem 1 proves for the model problem with Coulomb friction that the substitution of $\mathfrak{M}$ by appropriate smooth manifolds $\mathfrak{M}^{(\nu)}$ results in solutions tending to a unique limit for $\nu \to 0$ that is independent of the actual choice of $\mathfrak{M}^{(\nu)}$. This stable behaviour (based essentially on the monotonous derivative at $q_1 = 0$) makes phenomenological models of this kind attractive for numerical methods.

b) The crucial point in Theorem 1 is the monotonous (non-oscillating) change of v from v_- to v_+ for all trajectories passing the singularity. Observe that for a non-monotonous derivative we would obtain a dependence on the variation $\mathrm{Var}(\beta)$ rather than on $\Delta\beta = \beta - \beta_0$, this gives some insight into the reason for the non-uniqueness of a distributional solution.

Up to now we have not discussed how to define the smooth manifolds $\mathfrak{M}^{(\nu)}$. Obviously, for real-life applications a numerical method based on the above phenomenological approach will be efficient only if the constraints that define $\mathfrak{M}^{(\nu)}$ can be evaluated (very) fast. Several methods have been proposed by the authors of the present paper, among others spline approximations ([1]) and methods that are based on a smooth approximation of the absolute value ([9], [7]).

The solution $q(t)$ of (3) is not influenced by inactive unilateral constraints. Therefore it seems to be natural to base the definition of $\mathfrak{M}^{(\nu)}$ on the active constraints, only (as it was done defining the original constraint manifold $\mathfrak{M}$). In a model with contact conditions the active constraints correspond to the contact points in a rigid body contact model. To avoid singularities an elastic model is, however, much more favourable since it considers not only the contact *points* but the complete surfaces of the bodies being in contact to define contact *patches*. Therefore we use the complete (infinite) set of unilateral constraints (1) to determine $\mathfrak{M}^{(\nu)}$.

Instead of discussing this approach for general problems (3) we restrict ourselves to the special type of unilateral constraints that is characteristic of the model problem of Example 1 and the wheel-rail contact problem. In both cases we have $n_s = n_h$ and $S = [\underline{s}, \overline{s}]^{n_s}$ with $\underline{s}, \overline{s} \in \mathbb{R}$. For the wheel-rail contact problem n_s denotes the number of wheels in the system, for the model problem S simplifies to $[\underline{s}, \overline{s}]$ since $n_s = 1$. Furthermore the unilateral constraints (1) are of the specific form

$$0 \le h_i(q; s_i) = \varphi_i(q) - \zeta(s_i, \psi_i(q)) \ , \ \ (s_i \in [\underline{s}, \overline{s}] \ , \ i = 1, \ldots, n_h)$$

with $n_h = 1$,

$$\varphi_1(q) := q_2 \ , \ \ \psi_1(q) := q_1 \ , \ \ \zeta(s, q_1) := -\varrho \sin s + \sqrt{(q_1 + \varrho \cos s)^2 + a^2}$$

for the model problem (see (27)).

The constraint manifold $\mathfrak{M}$ is defined by (4), i. e. by $\min_{s_i} h_i(q; s_i) = 0$ or, equivalently, by

$$\varphi_i(q) = \max\nolimits_{s_i \in [\underline{s}, \overline{s}]} \zeta(s_i, \psi_i(q)) \ , \ \ (i = 1, \ldots, n_h) \ . \tag{28}$$

$\mathfrak{M}$ may have wedges since $\max_s \zeta$ is in general only continuous but not differentiable. We define the smooth manifolds $\mathfrak{M}^{(\nu)}$ as set of all $q \in \mathbb{R}^{n_q}$ satisfying

$$\varphi_i(q) = \mathrm{smax}^{(\nu)}_{s_i \in [\underline{s}, \overline{s}]} \zeta(s_i, \psi_i(q)) \ , \ \ (i = 1, \ldots, n_h) \tag{29}$$

with

$$\mathrm{smax}^{(\nu)}_{s \in [\underline{s}, \overline{s}]} \zeta(s, \psi) := \nu \ln \left(\frac{1}{\overline{s} - \underline{s}} \int_{\underline{s}}^{\overline{s}} \exp(\frac{1}{\nu} \zeta(s, \psi)) \, ds \right) \ . \tag{30}$$

It is verified straightforwardly that $\mathrm{smax}^{(\nu)}_s \zeta(s, \psi)$ defines a smooth function of ψ whenever $\nu > 0$ and $\zeta(s, \psi)$ is sufficiently often differentiable. Furthermore $\mathrm{smax}^{(\nu)}_s \zeta(s, \psi)$ converges pointwise to $\max^{(\nu)}_s \zeta(s, \psi)$ if $\nu \to 0$. This "smax–approach" can be extended to general problems of the form (3) but we omit this extension since it needs a lot of additional notations.

As an example Fig. 4 shows the constraint manifolds $\mathfrak{M}$ and $\mathfrak{M}^{(\nu)}$ with $\nu = 0.04$ for the model problem. Both in the smooth (left plot) and in the nonsmooth case (right plot) $\mathfrak{M}^{(\nu)}$ is a good approximation of $\mathfrak{M}$ if $\nu \ll 1$. The right plot illustrates that $\mathfrak{M}^{(\nu)}$ is differentiable even if $\mathfrak{M}$ is only continuous.

The phenomenological model that was discussed in detail for the model problem of Example 1 was successfully applied to the dynamical simulation of wheel-rail systems ([8], see also Sec. 5). On the one hand the new model preserves (approximately) the original model for

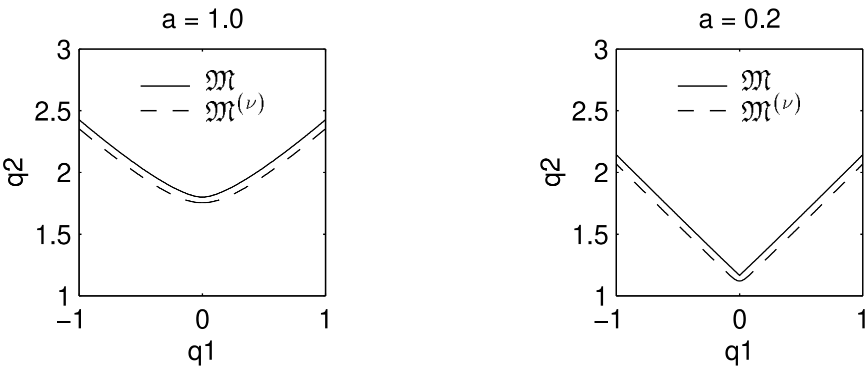

Figure 4: Projection of $\mathfrak{M}$ and $\mathfrak{M}^{(\nu)}$ on the (q_1, q_2)-plane, $(\varrho = 0.8,\ \nu = 0.04)$.

smooth branches. On the other hand it extends the original model to the nonsmooth case. This extension was defined such that it tends (at least for the model problem) to a well defined limit if the regularization parameter tends to zero. During the dynamical simulation the regularized constraints can be evaluated efficiently.

5 The dynamical simulation of wheel-rail systems with wear profiles

Rigid body contact models that are widely used in the dynamical simulation of wheel-rail systems yield model equations with unilateral constraints. If wheels with wear profiles (that are e. g. commonly used by the Deutsche Bahn AG) move on a standard track then these model equations can not be reduced to a DA-system with smooth constraints. In this section we sketch the geometrical problem of wheel-rail contact and apply the regularization technique of Section 4 to the model equations. Simulation results for a rigid wheelset in 2 typical benchmark problems illustrate the use of the proposed method in applied problems.

In the (elastic) contact of wheel and rail the shape of the contact patch is of great influence on the friction forces. However, in the geometrical contact condition the elastic deformation (that is in the range of 0.1 mm) may be neglected. This *rigid body contact model* avoids oscillations in the solution and saves up to 90% cpu-time compared with a pure elastic contact model. The geometrical contact conditions are formulated as (an infinite number of) unilateral constraints using the *profile functions* of wheel and rail. Throughout this section these profiles are given by the industrial standards UIC60-ORE (rail) and S1002 (wheel), for comparison with [21] we consider additionally conic wheels (wheels with linear profile function).

As basic unit of wheel-rail contact we use the contact of a single wheel and a rail. The relative position of wheel and rail is denoted by q_{rel}, we have $q_{\mathrm{rel}} \in \mathbb{R}^6$ corresponding to the 6 degrees of freedom. In a multibody system (MBS) model for the wheel-rail system this relative position is determined by the MBS coordinates q via several changes of coordinates, $q_{\mathrm{rel}} = q_{\mathrm{rel}}(q)$.

We proceed as in the 2D-case in Example 1 and define for all points on the wheel surface the elevation above the rail. If the wheel axle is perpendicular to the rail then the symmetry of the wheel enforces that all minima of this elevation are exactly below the centre of the wheel axle. This observation can be generalized to arbitrary q_{rel} ([3]): there is a line $\mathfrak{C} = \mathfrak{C}(q_{\mathrm{rel}})$ on the wheel surface such that wheel and rail do not penetrate each other iff no point of $\mathfrak{C}$ is below the rail surface. Instead of considering the two-dimensional wheel surface in the formulation of the contact condition we can therefore restrict ourselves to the one-dimensional line $\mathfrak{C}$. In general this line $\mathfrak{C}$ is parametrized by the wheel coordinate $s \in \mathbb{R}$ (the s-axis is parallel to the wheel axis) such that the contact condition can be formulated as

$$\delta(s, q_{\text{rel}}) \geq 0 \quad \forall\, s \in [\underline{s}, \overline{s}]$$

with an appropriate *distance function* δ (see [3] for the details). Furthermore, δ is defined such that the function

$$\zeta(s, q_{\text{rel}}) := \xi_z - \delta(s, q_{\text{rel}})$$

does not depend on the vertical displacement ξ_z of the wheel (that is one of the components of q_{rel}). Obviously, both δ and ζ depend on the profile functions of wheel and rail.

With the additional assumption (4) that wheel and rail are continuously in contact the ith wheel-rail contact defines a constraint

$$0 = g_i(q) := \xi_z^{(i)}(q) - \max_{s_i \in [\underline{s}, \overline{s}]} \zeta(s_i, q_{\text{rel}}^{(i)}(q)) \tag{31}$$

in the MBS model equations

$$\begin{aligned} M(q)\ddot{q} &= \varphi(t, q, \dot{q}, \lambda) - (\nabla_q g(q))^T \lambda \\ 0 &= g(q) \end{aligned} \tag{32}$$

for the wheel-rail system ($g = (g_1, \ldots, g_{n_h})^T$). Following the phenomenological model of Sec. 4 the regularized counterpart to (31) is obtained substituting $g(q) = 0$ by $g^{(\nu)}(q) = 0$ with $g^{(\nu)} = (g_1^{(\nu)}, \ldots, g_{n_h}^{(\nu)})^T$ and

$$0 = g_i^{(\nu)}(q) := \xi_z^{(i)}(q) - \operatorname{smax}^{(\nu)}_{s_i \in [\underline{s}, \overline{s}]} \zeta(s_i, q_{\text{rel}}^{(i)}(q)) \,. \tag{33}$$

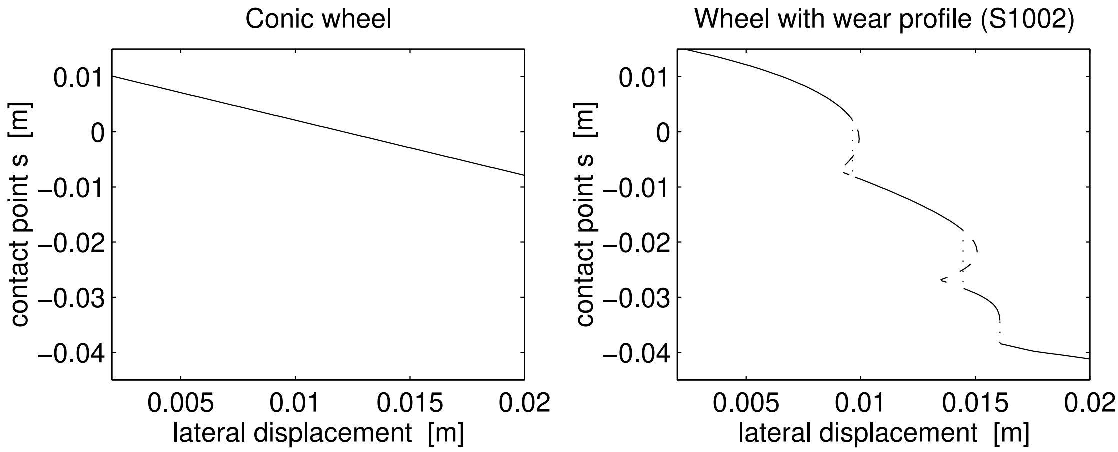

Figure 5: Contact point wheel-rail in nominal position (ξ_y varies).

For conic wheels equation (31) defines a smooth equality constraint $g = 0$ for all relative positions q_{rel} of practical interest. Therefore initial value problems for (32) are covered by the "smooth" case and may be solved by the techniques that were summarized in Section 2 (see also [21]). As in Fig. 3 we illustrate the smoothness of the constraint plotting the contact point(s), i. e. the point(s) s^* with

$$\zeta(s^*, q_{\text{rel}}) = \max_{s \in [\underline{s}, \overline{s}]} \zeta(s, q_{\text{rel}}(q)) \,, \tag{34}$$

versus one of the position coordinates $q_{\rm rel}$. In Fig. 5 we consider one wheel of a rigid wheelset in nominal position $q_{\rm rel}$ on a straight track and vary then the lateral displacement ξ_y of the wheel (ξ_y is one of the components of $q_{\rm rel}$). The left plot shows the smooth case (conic wheel), in the right plot we see 3 jumps of the contact point (marked by dotted lines) that are characteristic of wheels with wear profile. In general, each jump of the contact point corresponds to a configuration $q_{\rm rel}$ for that the constraints (31) are continuous but not differentiable. As in Fig. 3 we included dashed lines into the right plot showing all points s that are not contact points but satisfy the necessary condition $\frac{\partial}{\partial s}\zeta(s, q_{\rm rel}) = 0$ for a maximum in (34).

Remark 4 a) For wheels with wear profiles the jumps of the contact point are caused by the typical geometry of the wheel profile. In contrast to conic wheels we have to consider now wheels that consist of tread and flange. When the flange gets in contact with the rail the contact point jumps from $s \geq -32\,\mathrm{mm}$ (tread) to $s \leq -38\,\mathrm{mm}$ (flange). Within the tread the profiles of wheel and rail are approximately parallel because the wheel profile is defined on the basis of measured data from wheels that were a few $100,000\,\mathrm{km}$ in use (*wear* profile). Here, the contact point is the point of minimal distance between two nearly but not exactly parallel surfaces. As a result the contact point jumps not only between flange and tread but also within the tread.

b) Neglecting the elastic deformation totally we arrive at the nonsmooth constraints (31). Because of the discontinuities in the simulation results the error of this rigid body contact model may be very large (Example 4). The regularization (33) does also not take into account the *quantitative* effects of elastic deformation, but it considers this deformation *qualitatively*. Instead of focussing on the contact geometry in one single point ("the" contact point) it is based on the *global* contact geometry (corresponding to the contact *patch* in the real wheel-rail contact). We therefore call the application (33) of the regularization technique to contact problems the *quasi-elastic* contact model.

c) The optimal choice of the regularization parameter ν for problems of the general form (3) is an open problem since on the one hand large values of ν result in a large difference between the original and the regularized problem but on the other hand very small values of ν may cause numerical difficulties if the regularized problem is too close to the nonsmooth original problem. In the special case of model equations with contact conditions a natural choice of ν is motivated by the analogy between the quasi-elastic and a pure elastic model. For both models the rigid body contact conditions (31) are slightly violated (in the elastic model because of the elastic deformation and in the quasi-elastic model because of $\mathrm{smax}_s^{(\nu)}\zeta(s, q_{\rm rel}) \leq \max_s \zeta(s, q_{\rm rel})$). The parameter ν is chosen so that $\max_s \zeta - \mathrm{smax}_s^{(\nu)}\zeta$ is of the same size as the elastic approach in a pure elastic model (this elastic approach depends on the axle load, typical values are in the range of $10 \ldots 100\,\mu\mathrm{m}$.) For profiles S1002 (wheel) and UIC60–ORE (rail) appropriate values of ν are in the range $10^{-5} \ldots 5 \cdot 10^{-5}$, in the actual computations we used $\nu = 2 \cdot 10^{-5}$.

d) In the evaluation of function $g^{(\nu)}$ in (33) we use the same data ζ as in the computation of the friction forces that needs anyway this information about the geometry of wheel and rail surface within the contact patch. Thus, the fairly complicated structure of the constraints (33) does not result in an extraordinary additional numerical effort. Further savings are possible using instead of $g^{(\nu)}$ a spline approximation of $g^{(\nu)}$ in the dynamical simulation ([3]).

The new approach to the regularization of model equations with contact conditions has been applied to the dynamical simulation of real-life wheel-rail systems (see e. g. [3]), the results for 2 typical benchmark problems are shown below in Examples 3 and 4. We compare the quasi-elastic and the rigid body contact model, i. e. the regularized and the (possibly) nonsmooth constraints. For both models we use the BDF-code DASSL ([4]) applied to the Gear–Gupta–Leimkuhler formulation of the model equations (see also (16)). For algorithmic reasons it is important to use in the variable stepsize variable order computations instead of (33) an approximation of $\mathrm{smax}^{(\nu)}$ on a *fixed* grid $\underline{s} = s^{(0)} < s^{(1)} < \ldots < s^{(N)} = \overline{s}$

$$g_i^{(\nu)} := \xi_z^{(i)}(q) - \nu \ln\Big(\frac{1}{\overline{s} - \underline{s}} \sum_{j=1}^{N} \Delta s_i^{(j)} \ \exp(\frac{1}{\nu} \zeta(s_i^{(j)}, q_{\mathrm{rel}}^{(i)}(q)))\Big)$$

with $\Delta s_i^{(j)} := s_i^{(j)} - s_i^{(j-1)}$. We choose $\Delta s_i^{(j)} \approx 0.5\,\mathrm{mm}$ on the tread and $\Delta s_i^{(j)} \approx 0.2\,\mathrm{mm}$ on the flange of the wheel, i. e. for the wear profile S1002 one evaluation of $g_i^{(\nu)}$ uses $N \approx 200$ function values of ζ.

We compare our new model with the rigid body contact model of [17], [3] (in the smooth case (Example 3) this rigid body contact model is similar to the one in [21]). In the nonsmooth case (Example 4) we refer to simulation results that were originally presented in [3]. Here we combine the algorithm of Remark 1a) with an impact model from [13] that describes the jumps of velocity vector and Lagrange multipliers at the singularities of (31).

For both contact models Kalker's theory and his code FASTSIM ([15]) are used to compute the friction forces. However, in [17] the input of FASTSIM is based on the local contact geometry in the contact point instead of the global contact geometry that is used in the quasi-elastic model. This simplification is very useful for conic wheels ([21]) but introduces additional errors for wheels with wear profiles (Example 4, see also [1]).

Example 3 It is a well known phenomenon in railway engineering that the quasi-stationary motion of a rigid wheelset along a straight track gets unstable if the (fixed) speed exceeds a "critical" value (e. g. [14]). Consider a rigid wheelset with conic wheels moving with $V = 57\,\frac{\mathrm{m}}{\mathrm{s}}$ along a straight track. At $t = 0$ the wheelset is shifted by $y(0) = 20\,\mathrm{mm}$ in lateral direction, this results in a trajectory that does not tend to the nominal state ($y = 0$) but approaches a limit cycle with amplitude $y \approx 51\,\mathrm{mm}$. Eqs. (32) consist here of 6 second order differential equations and 2 equality constraints ([21]). As one simulation result the left plot of Fig. 6 shows the $(y, \dot{y})$ phase plot, the initial value is marked by the fat dot. Here in the smooth case the simulation results for rigid body and quasi-elastic contact model differ by a term of size $\mathcal{O}(\nu)$ that is smaller than the plot accuracy in the $(y, \dot{y})$–diagram. In the right plot of Fig. 6 that shows the vertical displacement z of the wheelset the difference between the simulation results is clearly visible. Wheel and rail as rigid bodies would touch for constraint (31), but for the quasi-elastic contact model (33) they would penetrate each other. The penetration ($\|g\| \approx 0.06\,\mathrm{mm}$) is in the same range as for a pure elastic model for contact steel–steel. Both rigid body and quasi-elastic contact model yield a DA-system with equality constraints, i. e. there are no high-frequency oscillations in the solution. However, the cpu-time for the quasi-elastic model is approximately 13.8 times larger than for the code of [17] because the distance function has to be evaluated much more often in (33), a motion of 10 s is simulated in 9.7 s and 133.8 s, respectively, on a Sparc5 workstation.

Example 4 ([3]) In simulation packages it has been popular to consider only the local contact geometry to simplify the computation of friction forces. For wheels with wear profile this approach results in large model errors in the neighbourhood of jumps of the contact point in Fig. 5. This is illustrated by a benchmark of [18]: A rigid wheelset moves with fixed speed along a straight track. It is shifted to the right ($y \approx 5.0\,\mathrm{mm}$) by a force $F_y = 20\,\mathrm{kN}$ acting in lateral direction. The motion tends to a quasi-stationary state that is at the right wheel very close to a configuration for that the contact point jumps from $-18\,\mathrm{mm}$ to $-28\,\mathrm{mm}$. Figs. 7 and 8 show

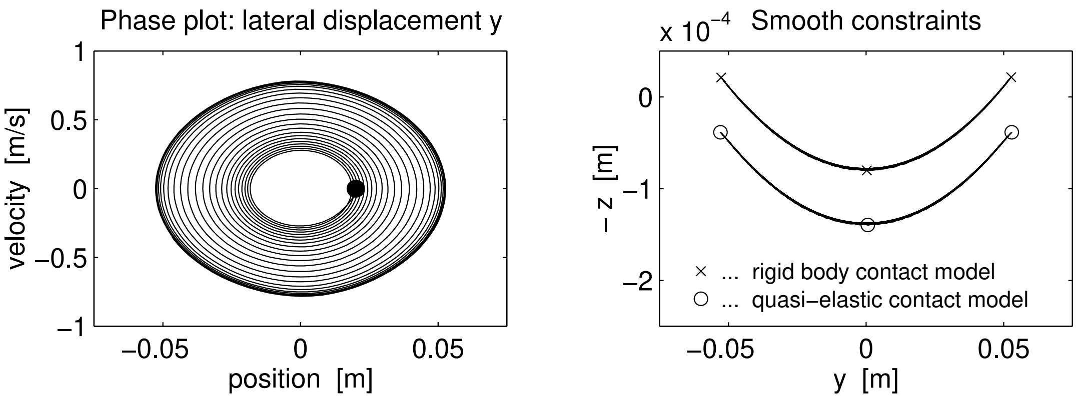

Figure 6: The smooth case (conic wheels): rigid wheelset moving with fixed speed $V = 57\,\frac{\mathrm{m}}{\mathrm{s}}$ along a straight track.

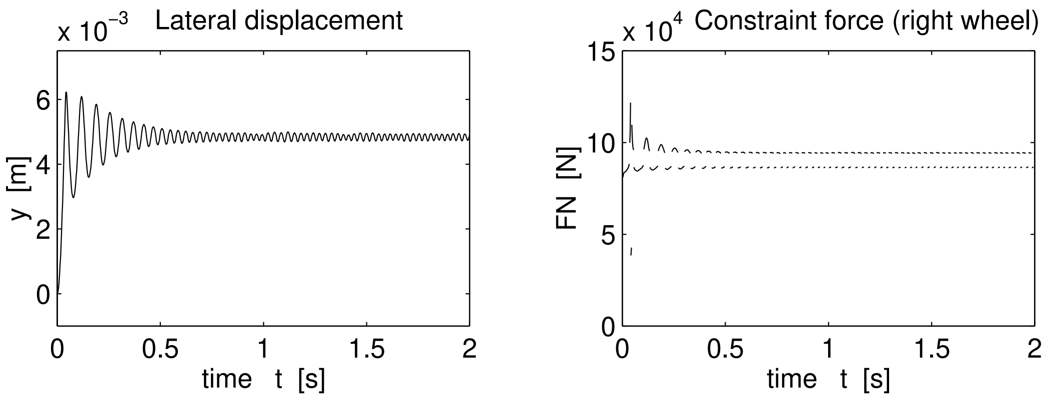

Figure 7: Nonsmooth contact conditions (wheels with wear profile): benchmark from [18].

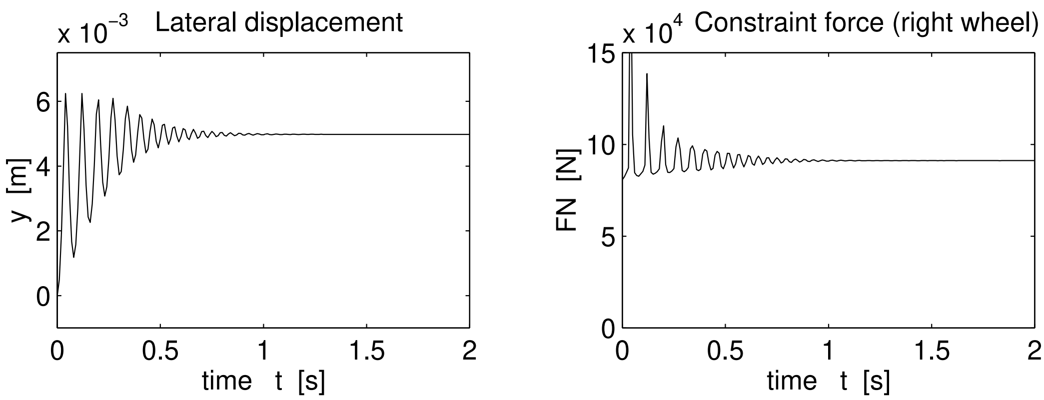

Figure 8: Regularized contact conditions (wheels with wear profile): benchmark from [18].

simulation results for the rigid body and the quasi-elastic contact model, respectively. Because of the nonsmooth constraints (31) the results in Fig. 7 do not tend to a quasi-stationary state but oscillate with frequent discontinuities in velocity vector and constraint forces. The rigid body contact model yields qualitatively wrong simulation results. The plots of Fig. 8 illustrate the benefits of the quasi-elastic contact model: the simulation results are in very good agreement with measured data, they approach the quasi-stationary state.

Summary

Time dependent problems with unilateral constraints may frequently be reduced to differential-algebraic systems that can be solved efficiently by DAE methods. In the present paper we discuss this approach in detail and focus on problems that result in differential-algebraic systems with non-differentiable constraints.

Based on the analysis of a simple model problem we define a regularization of the constraints that preserves the original model as long as the constraints are differentiable. In the case of non-differentiable constraints the model is extended in a way that is fairly independent of the regularization parameter ν since there exists a limit for $\nu \to 0$.

In the application to mechanical multibody systems with contact conditions this regularization defines the quasi-elastic contact model that was introduced as alternative both to the rigid and to pure elastic contact models. In the quasi-elastic model the contact conditions yield constraints that are sufficiently often differentiable such that standard DAE solvers can be applied efficiently. The quasi-elastic contact model is applied successfully in the dynamical simulation of wheel-rail systems.

Acknowledgement Part of this work has been done within the joint project "Differential equations and singular manifolds in the dynamical simulation of wheel-rail systems" of Rostock University and DLR Oberpfaffenhofen that is supported by the German Federal Minister for Education, Science, Research, and Technology (grant FR7ROK). We thank our colleagues in the wheel-rail groups in Rostock and Oberpfaffenhofen for very stimulating discussions about the topic of the present paper. The authors are especially grateful to Dipl.-Ing. H. Netter (Oberpfaffenhofen) who developed the simulation software that was used in Section 5.

References

[1] M. Arnold. The geometry of wheel–rail contact. In [6].

[2] M. Arnold. Numerical problems in the dynamical simulation of wheel-rail systems. *Z. Angew. Math. Mech.*, Proceedings of ICIAM 95, Issue 3:151–154, 1996.

[3] M. Arnold and H. Netter. Approximation of contact geometry in the dynamical simulation of wheel-rail systems. to appear in *Math. Modelling of Systems*, 1997.

[4] K.E. Brenan, S.L. Campbell, and L.R. Petzold. *Numerical solution of initial–value problems in differential–algebraic equations.* SIAM, Philadelphia, 2nd edition, 1996.

[5] E. Eich and C. Führer. *Numerical Methods in Multibody Dynamics.* Teubner – John Wiley, 1997, in preparation.

[6] K. Frischmuth, editor. *The dynamical simulation of wheel–rail systems, Proc. of the First Workshop on "Dynamics of Wheel–Rail–Systems", held at Rostock University (May, 5th and 6th, 1994)*, Universität Rostock, FB Mathematik, Preprint 94/21, November 1994.

[7] K. Frischmuth. Regularization methods for non-smooth dynamical problems. In R. Bogacz, G.-P. Ostermeyer, and K. Popp, editors, *Dynamical Problems in Mechanical Systems*, Polish Academy of Sciences, Warsaw, 1996.

[8] K. Frischmuth, M. Arnold, M. Hänler, and H. Netter. Differentialgleichungen und singuläre Mannigfaltigkeiten in der dynamischen Simulation von Rad–Schiene–Systemen. In K.-H. Hoffmann, W. Jäger, Th. Lohmann, and H. Schunck, editors, *Mathematik – Schlüsseltechnologie für die Zukunft*, pages 331–342. Springer-Verlag, Berlin Heidelberg New York, 1997.

[9] K. Frischmuth, M. Hänler, and St. Ostrzinski. On motion with non-smooth constraints. In [6].

[10] C. Führer. Private communication, 1992.

[11] C.W. Gear, G.K. Gupta, and B. Leimkuhler. Automatic integration of Euler–Lagrange equations with constraints. *J. Comp. Appl. Math.*, 12&13:77–90, 1985.

[12] E. Hairer and G. Wanner. *Solving Ordinary Differential Equations. II. Stiff and Differential-Algebraic Problems.* Springer-Verlag, Berlin Heidelberg New York, 1991.

[13] E.J. Haug, S.C. Wu, and S.M. Yang. Dynamics of mechanical systems with Coulomb friction, stiction, impact and constraint addition–deletion I. *Mechanism and Machine Theory*, 21:401–406, 1986.

[14] Ch. Kaas-Petersen. Chaos in a railway bogie. *Acta Mechanica*, 61:89–107, 1986.

[15] J.J. Kalker. *Three-Dimensional Elastic Bodies in Rolling Contact.* Kluwer Academic Publishers, Dordrecht Boston London, 1990.

[16] K. Knothe and S.L. Grassie. Modelling of railway track and vehicle/track interaction at high frequencies. *Vehicle Syst. Dyn.*, 22:209–262, 1993.

[17] H. Netter and M. Arnold. Geometrie und Dynamik eines Rad-Schiene-Modells in Deskriptorform mit unstetigen Zustandsgrößen. Technical Report IB 515–93–02, DLR, D-5000 Köln 90, 1993.

[18] J.P. Pascal. Benchmark to test wheel/rail contact forces. Technical report, INRETS Paris, 1990.

[19] P.J. Rabier and W.C. Rheinboldt. On the computation of impasse points of quasi-linear differential-algebraic equations. *Math. Comp.*, 62:133–154, 1994.

[20] W.C. Rheinboldt. On the existence and uniqueness of solutions of nonlinear semi-implicit differential-algebraic equations. *Nonlinear Anal., Theory Methods Appl.*, 16:647–661, 1991.

[21] B. Simeon, C. Führer, and P. Rentrop. Differential-algebraic equations in vehicle system dynamics. *Surveys on Mathematics for Industry*, 1:1–37, 1991.

[22] A.I. Volpert. The space BV and quasilinear equations (in Russian). *Matem. Sbornik. Akad. Nauk*, 73:225–302, 1967. English translation: Mathem. USSR–Sbornik, 2:225–267, 1967.